

# Monogenic Signal Theory Based Feature Similarity Index For Image Quality Assessment

<sup>1</sup>XUE-GANG LUO, <sup>2</sup>HUA-JUN WANG  
<sup>1,2</sup>School of Mathematics and Computer Science  
Panzhuhua University  
Sichuan Panzhuhua 617000  
CHINA

<sup>2</sup>Key Lab of Earth Exploration & Information Techniques of Ministry of Education  
Chengdu University of Technology  
Sichuan Chengdu 610059  
CHINA

[<sup>1</sup>lxg\\_123@foxmail.com](mailto:lxg_123@foxmail.com) [<sup>2</sup>21658388@qq.com](mailto:21658388@qq.com)

*Abstract:* -Image quality assessment (IQA) aims to establish generic metrics consistently with subjective evaluations using computational models. Recent phase congruency, which is a dimensionless, normalized feature of a local structure, is used as the structure similarity feature. This paper proposes a novel feature similarity (RMFSIM) index for full reference IQA based on monogenic signal theory. A monogenic phase congruency map, which is equipped to be relatively insensitive to noise variations, is constructed using phase, orientation and energy information of the 2D monogenic signal. The corresponding 1st-order and 2nd-order coefficients of the MPC map are obtained by Riesz transform. The local feature coefficients similarity is computed by the similarity measure and a single similarity score are combined together finally. Experimental results demonstrate that the proposed similarity index is highly consistent with human subjective evaluations and achieves good performance in terms of prediction monotonicity and accuracy.

*Key-Words:* - image quality assessment(IQA); monogenic phase congruency(MPC); human visual system; Feature Similarity Index

## 1 Introduction

Digital image suffers inevitably from a variety of distortions in the process of collection, processing, compression, storage, transmission. Due to the different levels of image quality decline, it is hard to obtain the real image. Numerous applications, such as image acquisition, image transmission, image compression, image restoration, and image enhancement, are being seriously affected. Therefore, image quality assessment (IQA) plays an important role in numerous computer vision and image process applications.

In general, there are two categorizations of IQA methods: subjective and objective ones. According to human visual system (HVS), subjective IQA metric, which is the most reasonable IQA metrics, estimates image quality by many observers to participate with image manually interpretation. However, it is not suitable for many important scenarios such as real-time and automated systems. Objective IQA method uses a mathematical model to calculate the similarity index by quantizing the distortion image and the reference image to obtain

the evaluation results, which a simple, easy IQA metric. There are some distinct advantages, for instance, embedding real time image processing system. According to the degree of dependence on the reference image, there are three categorizations of objective IQA methods: full reference (FR), reduce reference (RR) and non-reference type (NR). The traditional algorithms for full reference image quality assessment are Mean Squared Error (MSE) and Peak Signal-Noise Ratio (PSNR). Since these algorithms do not consider with the interdependence of pixels, the structure correlation between pixels and the characteristics of human visual perception, evaluation results of which are not consistent with subjective evaluation results, theirs results are unreliable for objective image quality assessment.

In order to achieve methods conform to human visual evaluation, a lot of evaluation methods based on visual characteristics were proposed, depending on sensitivity of the visual signals (such as brightness, contrast, spectrum) of the human visual system. The representative metrics are Visual Signal to Noise Ratio [1] and Visual Information

Fidelity[2]. Although these methods accord to the result of subjective evaluation, but it is still very limited to human understanding of HVS. The most popular method for FR-IQA is Structural Similarity index [3] (SSIM) by the luminance, contrast and structure comparison images obtained from the reference and distortion images. Experimental results demonstrate that it is more consistent with HVS than PSNR and MSE but less effective for badly blurred images. Recently, numerous extensions of SSIM have been developed, like Multi-Scale SSIM (MS-SSIM) index[4], complex wavelet structural similarity(CW-SSIM) index[5] and four-component SSIM[5], which to some extent improve the performance of measure. Feature-similarity (FSIM) index is proposed by Zhang et al. [6], which utilized the phase congruency (PC) as the primary feature and the gradient magnitude (GM) as the secondary feature to obtain the local quality map and weighted by PC to derive a single quality score. The performance of FSIM is superior to the performance of SSIM and the other variants by experimental results using six databases. However, phase congruency is highly sensitive to noise, the drawback of which has a strong impact on performance of FSIM.

In this paper, a novel feature similarity (MST-FSIM) index for full reference IQA is proposed based on monogenic signal theory by FSIM inspired. Firstly, a monogenic phase congruency map which is relatively insensitive to noise is presented, monogenic phase congruency instead of PC is considered as the primary feature. Then the corresponding 1st-order and 2nd-order feature coefficients of the MPC map are obtained by Riesz transform. The local feature coefficients similarity is computed by the similarity measure and a single similarity score are combined together finally. Experimental results demonstrate that the proposed similarity index is highly consistent with human subjective evaluations and achieves good performance in terms of prediction monotonicity and accuracy.

## 2 Monogenic Signal Theory

In this section, We now describe briefly the main theory on which the algorithms proposed in the paper are based.

### 2.1 Riesz transform

The Hilbert transform of a 1-D function has been widely used in signal processing since Gabor proposed the analytic signal. The Hilbert transform  $H[g(t)]$  of a signal  $g(t)$  is defined by the following convolution integral [7]:

$$H[g(t)] = g(t) * \frac{1}{\pi t} \rightarrow -j \operatorname{sgn}(\omega) G(\omega) \quad (1)$$

Where  $*$  stands for the convolution, FT means Fourier transform,  $G(\omega)$  is the Fourier transform of  $g(t)$  and  $\operatorname{sgn}(\omega)$  is the sign function. However, problems occur in image processing applications are based on 2-D signal processing. The Riesz transform is the natural multidimensional signal representation of the 1-D Hilbert transform [8]. It is the scalar-to-vector signal transformation whose frequency response is  $-j\omega / \|\omega\|$ . In 2-D space, given the input signal  $f(x)$  with  $x = \{x_1, x_2\}$ , by using the well-known property that  $G\{1/\|x\|\}(\omega) = 2\pi / \|\omega\|$  and performing a partial differentiation with respect to  $x_1$  or  $x_2$ , we readily derive the corresponding impulse responses  $R_{x_1} = x_1 / 2\pi \|x\|^3$  and  $R_{x_2} = x_2 / 2\pi \|x\|^3$ ,  $f_R(x)$  by Riesz transform can be expressed as

$$f_R(x) = \begin{pmatrix} R_{x_1} * f(x) \\ R_{x_2} * f(x) \end{pmatrix} = \begin{pmatrix} \frac{x_1 f(x)}{2\pi(x_1^2 + x_2^2)^{\frac{3}{2}}} \\ \frac{x_2 f(x)}{2\pi(x_1^2 + x_2^2)^{\frac{3}{2}}} \end{pmatrix} \quad (2)$$

$$\begin{cases} R_{x_1 x_2}(f) = R_{x_1} * R_{x_2}(f) \\ R_{x_1 x_1}(f) = R_{x_1} * R_{x_1}(f) \\ R_{x_2 x_1}(f) = R_{x_2} * R_{x_1}(f) \end{cases} \quad (3)$$

In order to analyze i2D image structures, higher order Riesz transforms [9] are utilized to get important features of monogenic phase congruency. Therefore, in our metric, the coefficients of the 1st-order and the 2nd-order Riesz transform are extracted. The 1st-order Riesz transform  $R_{x_1}(f), R_{x_2}(f)$  can be obtained with Eq.(2), the 2nd-order Riesz transform  $R_{x_1 x_1}(f), R_{x_1 x_2}(f),$

$R_{x_2 x_2}(f)$  can be obtained with Eq. (3).

### 2.2 Monogenic signal

The monogenic signal which is the third generalization of the analytic signal was introduced by Felsberg in 2001[10]. It is considered to be a multi-dimensional extension of the analytic signal. For an image  $f(x)$ , the monogenic signal  $\mathbf{f}_m$  is defined as the combination of  $f$  and its Riesz transform.

$$\mathbf{f}_m(x) = \{f(x), R_{x_1} * f(x), R_{x_2} * f(x)\} \quad (4)$$

The local amplitude (energy) and local phase of  $f(x)$  over scale  $s$  are given by

$$\begin{aligned} \mathbf{A}_s(x) &= \|\mathbf{f}_m(x)\| \\ &= \sqrt{f_s^2(x) + (R_{x_1} * f_s(x))^2 + (R_{x_2} * f_s(x))^2} \end{aligned} \quad (5)$$

$$\varphi_s(x) = -\text{sign}(R_{x_1} * f_s(x)) a \tan 2 \left( \frac{R}{f_s(x)} \right) \quad (6)$$

Where  $R = \sqrt{(R_{x_1} * f_s(x))^2 + (R_{x_2} * f_s(x))^2}$ .

The local orientation over scale  $s$  can be calculated as

$$\theta_s(x) = a \tan 2 \left( \frac{R_{x_2} * f_s(x)}{R_{x_1} * f_s(x)} \right) \quad (7)$$

The monogenic signal has a representation that is invariant and equivariant with respect to energetic and structural information, which is the orthogonal decomposition of the 2-D image by Quadrature (mirror) filters. Since energy and structure are independent information, the local phase only changes if the local structure varies, structural information is invariant with respect to the local energy of the signal. In contrast, the local amplitude is invariant with respect to the energetic information but represents the local energy [10].

### 2.3 Monogenic phase congruency

Phase congruency is a method for feature detection that is different from the method based on gradient in spatial domain, which can only detect step features, phase congruency correctly detects features at all kind of phase angle, and not just step features having a phase angle of 0 or 180 degrees. Features of signals correspond to those points where phase congruency or similarity is maximum using the phase information of signals. It is immune to illumination and contrast for feature detector.

Denote by  $M_s^e$  and  $M_s^o$  the even- and odd-symmetric filters on scale  $s$ , and they form a quadrature pair. Responses of each quadrature pair to the signal will form a response vector at position  $x$  on scale  $s$ :  $[e_s(x), o_s(x)] = [f(x) * M_s^e, f(x) * M_s^o]$ , so the local amplitude is  $A_s(x)$  and is expressed as  $\sqrt{(e_s(x))^2 + (o_s(x))^2}$ , and the term  $E(x)$  is the local energy function and

is expressed as  $\sqrt{(\sum_s e_s(x))^2 + (\sum_s o_s(x))^2}$ . In this paper, the log-Gabor filters is adopted to  $e_s(x)$  and  $o_s(x)$  for the expansion of two-dimensional image. Eq.(7) is the definition of the phase congruency over orientation  $\theta$  and scale  $s$ .

$$PC(x) = \frac{\sum_{\theta} [E(x) - T_{\theta}]}{\varepsilon + \sum_{\theta} \sum_s A_s(x)} \quad (8)$$

Where  $\varepsilon$  is a small positive constant,  $\theta$  indicates the direction and  $[ ]$  denotes that the enclosed quantity is not permitted to be negative.  $T_{\theta}$  compensates for the influence of noise and is estimated empirically. Fig.1 shows the phase congruency maps calculated from a reference and distorted image (distorted with additive white Gaussian noise) from LIVE database. The noise present in the image (Fig. 1(e)) is creating a visual disturbance. The main reason is some amount of noise causing the high energy is removed in the definition of phase congruency given in Eq.(7). However, such noise is also responsible for the changes in the denominator incorporating  $\sum_{\theta} A_s(x)$ . But the denominator remains unchanged.



(a) original image



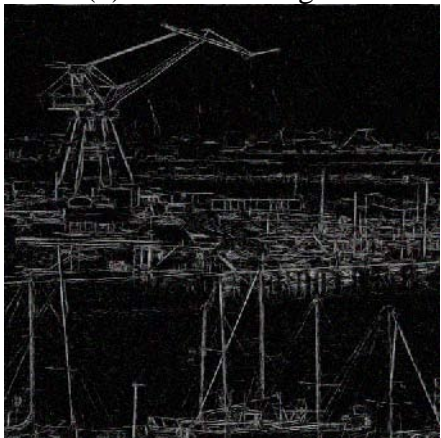
(b) PC of original image



(c) MPC of original image



(d) distorted image



(e) PC of distorted image



(f) MPC of distorted image

Fig. 1. (a) and (d) original image and corresponding distorted image with additive white Gaussian noise; (b) and (e) Phase congruency maps corresponding to (a) and (d), resp; (c) and (f) Monogenic phase congruency corresponding to (a) and (d), resp.

To improve performance in distortion wise perceptual analysis, we present a new measure of phase congruency based on the monogenic signal. The 2-D image using monogenic signal developed by Felsberg [10] is decomposed into three orthogonal components of local amplitude, local phase and local orientation. This measure approximates Based on the theory that phase congruency can be determined by the local maximum of amplitude, monogenic phase congruency is proposed, which can be expressed as:

$$MPC_s(x) = W(x) \left[ 1 - factor \times a \cos\left(\frac{E'(x)}{A'(x)}\right) \right] \frac{|E'(x) - T|}{A'(x) + \varepsilon} \quad (9)$$

Where  $W(x)$  is a weighting function that is constructed by applying a sigmoid function to the filter response spread value.  $factor$  is a factor from 1 to about 2, which acts to sharpen up the edge response.  $T$  is kept the same as Eq.(7). The summation of local energetic information is defined by Eq.(10). Eq.(11) defines the summation of local amplitude.

$$E'(x) = \sqrt{fs^2 + fr_{x_1}^2 + fr_{x_2}^2} \quad (10)$$

Where  $fs = \sum_s f_s(x)$ ,

$$fr_{x_1} = \sum_s (R_{x_1} * f(x)),$$

$$fr_{x_2} = \sum_s (R_{x_2} * f(x))$$

$$A'(x) = \sum_{s=1}^n A_s(x) \quad (11)$$

Comparison and analysis from Eq.(8) and Eq.(9), rather than use dot and cross products it is simpler and more efficient to simply use  $a \cos(\frac{E'(x)}{A'(x)})$  to obtain the weighted phase deviation directly in monogenic phase congruency. The value below the noise threshold is not subtracted from energy immediately as this would interfere with the phase deviation computation. Instead it is applied as a weighting as a fraction by which energy exceeds the noise threshold.  $W(x)$  is applied in addition to the weighting for frequency spread. Monogenic phase congruency has excellent speed and much reduced memory requirements compared to the other phase congruency functions.

### 3 Riesz transform based monogenic phase congruency feature similarity index

In this section, we will describe the proposed Riesz transform based monogenic phase congruency feature similarity index called RMFSIM.

Given a reference image  $f$  and a distorted image  $g$ , the general scheme of RMFSIM is shown in Fig.2. Let  $R_1, R_2$  and  $R_3$  represent three orthogonal components of local amplitude, local phase and local orientation of monogenic signal of the image. Let  $R_4, R_5$  represent the 1st order Riesz transform coefficients and  $R_6, R_7, R_8$  represent the 2nd-order coefficients of monogenic phase congruency of the image. The feature similarity of  $f$  and  $g$  is calculated as:

$$R_n^{sim} = \frac{2R_n^f R_n^g + \varepsilon_n}{(R_n^f)^2 + (R_n^g)^2 + \varepsilon_n} \quad (12)$$

Where  $n$  is a subscript, which is the  $n$ th feature coefficients map.

The RMFSIM will be calculated as follows six steps:

1. Change both images from RGB color space into gray scale for simplicity in this paper. This can apply equally to other color space, for instance HSV, CLE Lab. Even the color information can also be used.
2. Calculate the monogenic signal of both gray images to obtain the local amplitude, local phase and local orientation of monogenic signal of the image using Eqs.(5) (6) and (7). Because of three components be orthogonal, they can represent image

features. Therefore, make use of Eqs.(12), image feature maps of  $R_1^{sim}, R_2^{sim}$  and  $R_3^{sim}$  are obtained.

3. Utilize Eqs.(9) to figure out monogenic phase congruency of both the reference image and the distorted image.

4. Instead of phase congruency, uses monogenic phase congruency to get the coefficients of the 1st-order and the 2nd-order Riesz transforms. Make use of Eqs.(12) to form monogenic phase congruency feature maps of  $R_1^{sim}, R_2^{sim}, R_3^{sim}, R_4^{sim}$  and  $R_5^{sim}$ .

5. Combine eight feature maps into a signal feature map with the weighting factors, calculate the normalized feature map with Eqs.(14), scale the final feature map between 0 and 1.

$$FSIM(f, g) = \sum_{i=1}^8 \omega(i) \cdot R_i^{sim} \quad (13)$$

$$NormalFSIM(f, g) = \frac{FSIM(f, g)}{\max(FSIM(f, g))} \quad (14)$$

Where  $\omega(i)$  are the weighting factors to get a higher score of Spearman's Rank-Order Correlation Coefficient and  $\sum_{i=1}^8 \omega(i) = 1$ . For simplicity,  $\omega(i) = 1/8$  for this paper.

6. Calculate the RMFSIM value, which is the final score of the distorted image

$$RMFSIM(f, g) = \frac{\sum NormalFSIM(f, g)}{size(g)} \quad (15)$$

Where  $size(g)$  is the size of the distorted image  $g$ .

Through combining the coefficients maps of the 1st-order and the 2nd-order Riesz transforms of monogenic phase congruency with image feature maps, the RMFSIM value on same scale is obtained. It is easy to integrate the proposed feature similarity index with the thinking of multi-scale into the novel multi-scale feature similarity index.

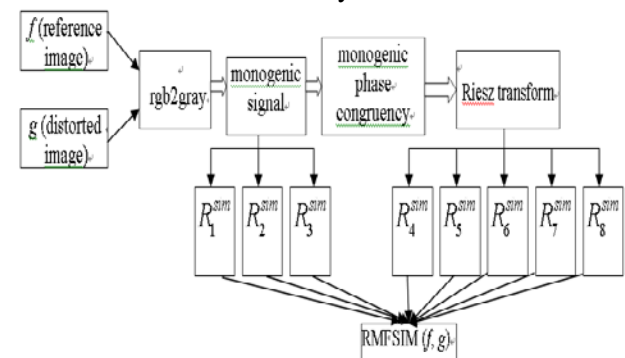


Fig. 2. General scheme of the proposed RMFSIM index.

## 4 Experimental results and analysis

In this section, in order to test the performance of our quality assessment algorithm, we choose publicly available databases. The first one is provided by the Laboratory for Image & Video Engineering (LIVE) of the University of Texas Austin, called LIVE database which contains 29 high-resolution (typically 768\*512) original images and a number of images distorted with different distortion types. The second one is TID2008 database which contains 1700 test images (25 reference images, 17 types of distortions for each reference image, 4 different levels of each type of distortion). Mean Opinion Scores (MOS) for LIVE and TID2008 database have been obtained. The experimental results of the proposed RMFSIM compare with other famous metrics including PSNR, SSIM[3], VIF [2], MS-SSIM [4], FSIM [6], FSIM<sub>c</sub> [6], IW-SSIM[11] on LIVE[12], TID2008 [13] image database.

The parameters for computing monogenic phase congruency are kept same as in the implementation by Kovsi. The value of  $\varepsilon_n$  in Eq.(8) is set to 0.002, and the value of *factor* in Eq.(9) is fixed to 1.5.

### 4.1 Evaluation measures

In our experiments, we have used five evaluation metrics for the quantitative analysis of the proposed method. These evaluation measures are shown in the following.

- (1) Spearman's Rank Correlation Coefficient (SRCC), which is a nonparametric rank-based correlation metric, independent of any monotonic nonlinear mapping between subjective and objective scores.
- (2) Kendall's Rank Correlation Coefficient (KRCC), which is another nonparametric rank correlation metric [11].
- (3) Pearson's Linear Correlation Coefficient (PLCC), which provides a non-linear mapping between the subjective and objective scores.
- (4) Mean Absolute Error (MAE), which is calculated using the converted objective scores after the nonlinear mapping.

- (5) Root Mean Square Error (RMSE), which is a metric that is similar to MAE.

A better objective IQA measure should have higher PLCC, SRCC, and KRCC while lower MAE and RMSE values. For PLCC, MAE and RMS, a 5-parameter logistic function is used for mapping between the subjective and objective scores. The logistic function is given by

$$PQ(x) = \lambda_1 \left( \frac{1}{2} - \frac{1}{1 + \exp(\lambda_2(x - \lambda_3))} \right) + \lambda_4 x + \lambda_5 \quad (14)$$

where  $\lambda_1, \lambda_2, \lambda_3, \lambda_4$  and  $\lambda_5$  are the five parameters to be fitted with a nonlinear regression process. The logistic transform is used to bring the objective scores in a common ground with the DMOS/MOS by providing a non-linear mapping between them.

### 4.2 Overall performance comparison

In this subsection, the experimental results of RMFSIM are compared with other IQA metrics, which contain PSNR, SSIM, VIF, MS-SSIM, FSIM, FSIM<sub>c</sub>, IW-SSIM. For PSNR, SSIM, VIF and MS-SSIM, we use the code provided by website, which is available at [12], for FSIM and IW-SSIM, we use the implementation provided by the author.

Table 1 lists the score of SRCC, KRCC, PLCC, MAE and RMSE of all IQA metrics on LIVE and TID2008 database, and the best two are highlighted in boldface. From Table 1 we can see that the performance of RMFSIM is quite nice, it get rival scores on LIVE and TID2008. Meanwhile, it is noteworthy that VIF perform fairly well on LIVE database, but the performance of it is quite poor on TID2008 database, and the performance of FSIM and FSIM<sub>c</sub> is better than other metrics except for RMFSIM on TID2008 database. However, the performance of RMFSIM is slightly better than the performance of FSIM and FSIM<sub>c</sub>. To improve performance on all IQA databases, our method is inspired by features of image for general measure. Scatter plots of objective scores vs. MOS for all metrics on TID2008 database, along with the best nonlinear fitting according to Eq.(14) are shown in Fig.3. We can see that the points of RMFSIM and FSIM<sub>c</sub> are closer to fitted curves, which means that the performance of feature similarity index is better than other metrics.

Table 1. Performance comparison of IQA metrics on LIVE and TID2008 database

Database	Metrics	PSNR	SSIM	VIF	MS-SSIM	FSIM	FSIM <sub>c</sub>	IW-SSIM	RMFSIM
LIVE	SRCC	0.8756	0.9482	<b>0.9714</b>	0.9513	0.9634	0.9645	0.9566	<b>0.9702</b>
	KRCC	0.6865	0.8159	<b>0.8548</b>	0.8026	0.8346	0.8345	0.8198	<b>0.8427</b>
	PLCC	0.8723	0.9448	<b>0.9653</b>	0.9489	0.9597	<b>0.9613</b>	0.9519	0.9602
	MAE	10.5674	7.5724	6.0412	6.6701	<b>5.8301</b>	5.9236	6.3805	<b>5.8209</b>
	RMSE	13.4583	6.1436	<b>4.8797</b>	8.6143	7.6705	7.5236	8.3757	<b>5.8679</b>
	SRCC	0.5245	0.6256	0.7496	0.8528	0.8805	<b>0.8840</b>	0.8559	<b>0.8809</b>
TID2008	KRCC	0.3696	0.4531	0.5863	0.6543	<b>0.6946</b>	<b>0.6991</b>	0.6636	0.6901
	PLCC	0.5545	0.6410	0.8025	0.8419	0.8733	<b>0.8758</b>	0.8572	<b>0.8742</b>
	MAE	0.8918	1.0299	0.8006	0.5616	0.4912	<b>0.4868</b>	0.5245	<b>0.4906</b>
	RMSE	1.1168	0.8215	<b>0.6060</b>	0.7247	0.6543	0.6482	0.6915	<b>0.6231</b>

### 4.3 Performance on individual distortion types

To further examine the effects of the proposed method, it is crucial enough to demonstrate the performance of RMFSIM on different distortions. Therefore, we present the performance of all metrics on five distortion types of LIVE database and make comparisons.

The evaluation results of the above IQA metrics and our own RMFSIM are summarized in Table 2 using SROCC. Higher values of SROCC indicate that the assessment method is better. In the table,

the top two performances for each distortion type in LIVE database are highlighted in bold and underline.

It's not hard to make out that RMFSIM has greater generalization ability exhibited by Table 2 than the other measures. For three of five distortion types, VIF lies within the top two performers. Also, we notice that IW-SSIM performs well for blur images. Though RMFSIM is not among the top two measures for blur distortion type, it is indeed very close to the second best. Therefore, it is obvious that overall performance on individual distortion types of RMFSIM is superior to the other metrics.

Table 2. Distortion-wise performance comparison using SROCC in LIVE database.

Database	Distortion type	PSNR	SSIM	VIF	MS-SSIM	FSIM	FSIM <sub>c</sub>	IW-SSIM	RMFSIM
LIVE	jp2k-comp	0.8954	0.9614	0.9696	0.9628	0.9716	<b>0.9723</b>	0.9649	<b>0.9719</b>
	jpeg-comp	0.8809	0.9764	<b>0.9846</b>	0.9814	0.9834	0.9840	0.9808	<b>0.9842</b>
	wn	<b>0.9854</b>	0.9694	0.9807	0.9733	0.9652	0.9716	0.9667	<b>0.9822</b>
	blur	0.7823	0.9517	<b>0.9728</b>	0.9543	0.9707	0.9709	<b>0.9719</b>	0.9690
	trans-error	0.8907	0.9556	<b>0.9650</b>	0.9471	0.9499	0.9520	0.9442	<b>0.9529</b>

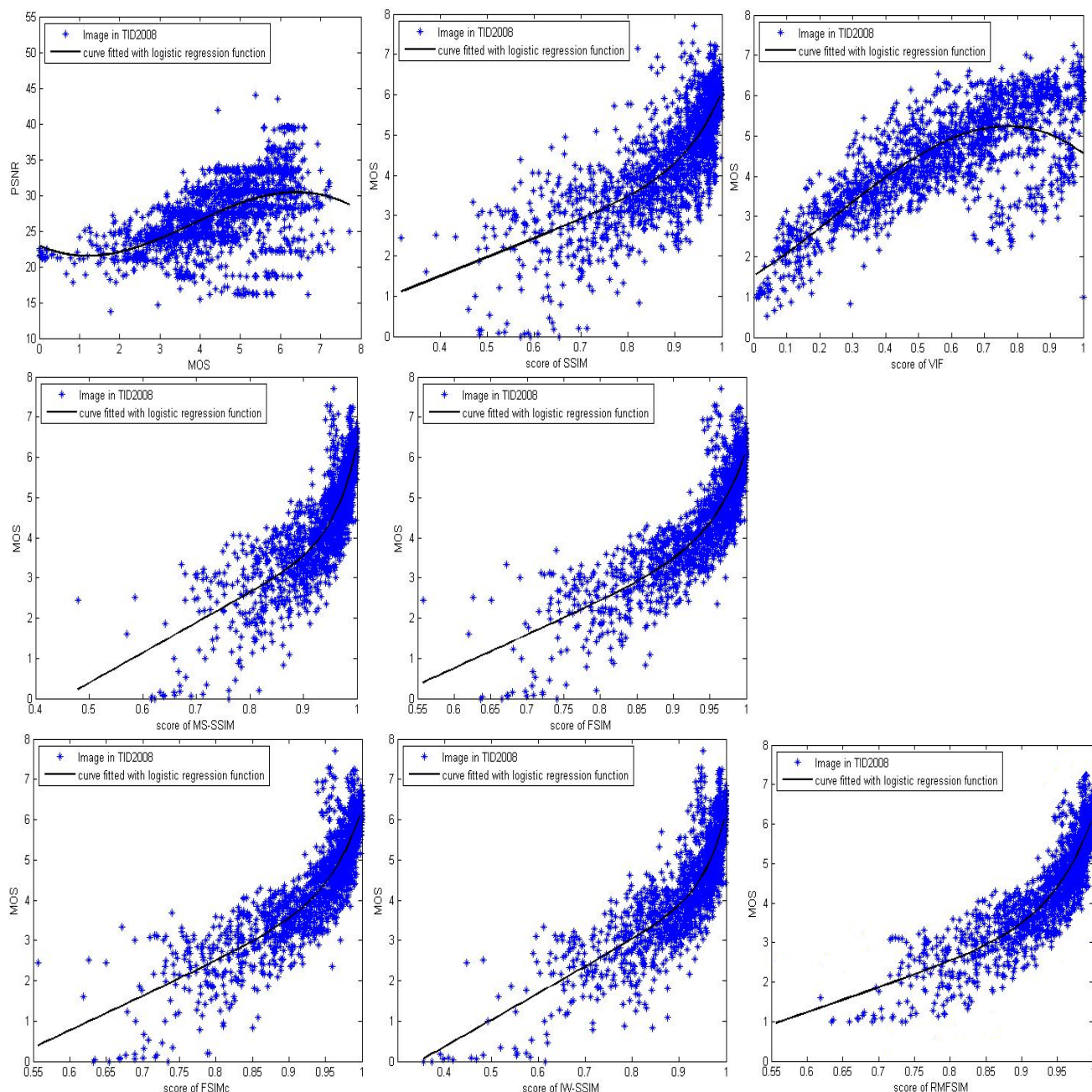


Fig.3. Scatter plots of subjective MOS versus scores obtained by model prediction on the TID2008 database.

### 5 Conclusion

Full reference image quality assessment using phase congruency based image features is successful. However, the phase congruency algorithm is less sensitive to noise depending on the noise removal technique used. This paper proposed a novel feature similarity index for image quality assessment based on monogenic signal theory. Monogenic phase congruency, which has the better ability of resisting noise interference than the traditional phase congruency, is presented. We combine the coefficients maps of the 1st-order and the 2nd-order Riesz transforms of MPC

with image feature maps of monogenic signal to evaluate perceptual quality of images.

Compared to the existing state-of-the-art approaches, the proposed method exhibited improved performance in distortion wise perceptual analysis. The method also demonstrated better generalization performance than its nearest competitors. RMFSIM is highly consistent with human subjective evaluations and achieves good performance in terms of prediction monotonicity and accuracy.

*References:*

- [1] Chandler D M, Hemami S S. VSNR: A wavelet-based visual signal-to-noise ratio for natural images[J]. *Image Processing, IEEE Transactions on*, 2007, 16(9): 2284-2298.
- [2] Sheikh H R, Bovik A C. Image information and visual quality[J]. *Image Processing, IEEE Transactions on*, 2006, 15(2): 430-444.
- [3] Wang Z, Bovik A C, Sheikh H R, et al. Image quality assessment: From error visibility to structural similarity[J]. *Image Processing, IEEE Transactions on*, 2004, 13(4): 600-612.
- [4] Wang Z, Simoncelli E P, Bovik A C. Multiscale structural similarity for image quality assessment[C]//*Signals, Systems and Computers, 2003. Conference Record of the Thirty-Seventh Asilomar Conference on. IEEE, 2003, 2: 1398-1402.*
- [5] Sampat M P, Wang Z, Gupta S, et al. Complex wavelet structural similarity: A new image similarity index[J]. *Image Processing, IEEE Transactions on*, 2009, 18(11): 2385-2401.
- [6] Zhang L, Zhang L, Mou X, et al. FSIM: a feature similarity index for image quality assessment[J]. *Image Processing, IEEE Transactions on*, 2011, 20(8): 2378-2386.
- [7] E. Stein and G. Weiss, *Introduction to Fourier Analysis on Euclidean Spaces*. Princeton, NJ: Princeton Univ. Press, 1971.
- [8] O. Fleischmann, *2D signal analysis by generalized Hilbert transforms*, Thesis, University of Kiel, 2008.
- [9] M.C. Morrone, R.A. Owens, Feature detection from local energy, *Pattern Recognition Letters* 6 (5) (1987) 303–313.
- [10] Felsberg M, Sommer G. The monogenic signal[J]. *Signal Processing, IEEE Transactions on*, 2001, 49(12): 3136-3144.
- [11] Zhou Wang and Qiang Li, Information Content Weighting for Perceptual Image Quality Assessment, *IEEE Transactions on Image Processing*, vol. 20, no. 5, pp. 1185–1198, May 2011.
- [12] H. R. Sheikh, K. Seshadrinathan, A. K. Moorthy, Z. Wang, A. C. Bovik and L. K. Cormack, Image and video quality assessment research at LIVE, [Online]. Available: <http://live.ece.utexas.edu/research/quality/>
- [13] N. Ponomarenko, V. Lukin, A. Zelensky, K. Egiazarian, M. Carli and F. Battisti, "TID2008- A database for evaluation of full-reference visual quality assessment metrics," *Advances of Modern Radioelectronics*, vol.10, pp. 30-45, 2009.